Enhanced Inverted Perovskite Solar Cell Performance via Ternary Bottom Passivation Layer Strategy

Li-Chun CHANG[1], Anh Dinh Bui[1], Keqing Huang[1], Wei Wang[1], Anne Haggren[1], Xuan Minh Chau Ta[2], Leiping Duan[1], Olivier Lee Cheong Lem[3], Viqar Ahmad[1], Daniel Walter[1], Klaus Weber[1], Kylie Catchpole[1, *], Heping Shen[1, *]

[1] School of Engineering, The Australian National University, Canberra, Australian Capital Territory, 2601 Australia.

[2] School of Chemistry, The Australian National University, Canberra, Australian Capital Territory, 2601 Australia.

[3]Research School of Physics, The Australian National University, Canberra, Australian Capital Territory, 2601 Australia.

Introduction

Among different Perovskite solar cells (PSCs) structures, p-i-n structure possesses key advantages such as superior stability, minimal hysteresis, competitive efficiency, positioning it as a promising structure for future practical applications. [1] Over the last decade, despite the stunning progress of the powever conversion efficiency (PCE) of inverted PSC, which achieves an impressive certified 25.4%.[2] Additionally, it has exhibited outstanding stability performance, including retaining 95% of its initial efficiency following over 1000 hours of exposure to damp-heat test conditions[3]. However, the performance of the cell in inverted structure still lags behind that of their regular counterparts in n-i-p structrue, primarily due to a lower open-circuit voltage (V_{OC}) and fill factor (*FF*) [4]. The losses are mainly at the interfaces between the perovskite and the carrier transport layer (CTL), wherein carrier recombination may occur on both the perovskite/electron transport layer (ETL) and hole transport layer (HTL)/perovskite interfaces. There has been extensive research focusing on PVK/ETL interface[5] while bottom interface has been understudied owing to the potential wash-off of introduced materials by the perovskite solution solvent. In addition, amorphous regions and voids can be created on the bottom interface by the initial evaporation of entrapped PbI_2-Dimethylsulfoxide (DMSO) intermediate phase during the crystallization process.[6] The interface recombination loss is highly dependent on the selected hole transport materials (HTMs).

Among various organic HTMs, Poly(N,N'-bis(4-butylphenyl)-N,N'-bis(phenyl)benzidine) (Poly-TPD) is promising due to its high hole mobility ($1 \times 10^{-4}\ cm^2V^{-1}s^{-1}$), resistance to polar solvents, and an appropriate energy level (HOMO:−5.4eV and LUMO:−2.4 eV), making it suitable for high bandgap perovksite solar cells.[7] Nevertheless, the relatively poor wettability of this polymer impairs the coverage of the perovskite film, subsequently exacerbating non-radiative recombination loss at the interface.[8] Different strategies have been explored to address this issue, solvent-additive engineering,[9] molecular weight control, and interlayer treatment.[8] Among these, interlayer treatment has gained notable precedence due to its high reproducibility and the advantageous role it plays in perovskite passivation. Poly(9,9-bis(3'-(N,N-dimethyl)-N-ethylammoinium-propyl-2,7-fluorene)-alt-2,7-(9,9-dioctylfluorene))dibromide (PFN-Br) has been commonly used between the HTL polymer and the perovskite absorber.[10] However, a notable issue is its tendency to relocate to the top of the absorber film during the perovskite growth process, leading to a deficiency in bottom passivation beneath the perovskite.[11] Apart from the wettability issue on the bottom side, the passivation at the PVK/HTL interface is hard to reproduce and control due to the high solubility of common passivation molecules in the perovskite precursor solvent. [12]

In the present study, we treated the Poly-TPD HTL with a ternary modulation layer comprising different ammonium salts (Phenethylammonium chloride [PEACl], 4-Methylphenethylammonium chloride [4M-PEACl], and n-Octylammonium Chloride [n-OACl]), Methylammonium iodide (MAI) and

a polyelectrolyte (PFN-Br) which boosted the performance of inverted-structure PSC. We discovered that the 4M-PEACl salt outperforms other salts, which could be attributed to the strong electron-withdrawing benzene ring that passivates undercoordinated Pb^{2+} ions. We observed the improvemet of the wettability on the interface, leading to a consecutive vertical growth of perovskite. We observed that adding MAI assists in modulating the 2D perovskite phase that forms at the bottom interface.[13] Meanwhile, we observed enhanced light stability on the bottom interface modificated deivices which remained on average 92.5% initial PCE after 550 hours continuous 1-sun illumination. This method significantly enhances both the efficiency and stability of the inverted PSCs.

Results & Discussion

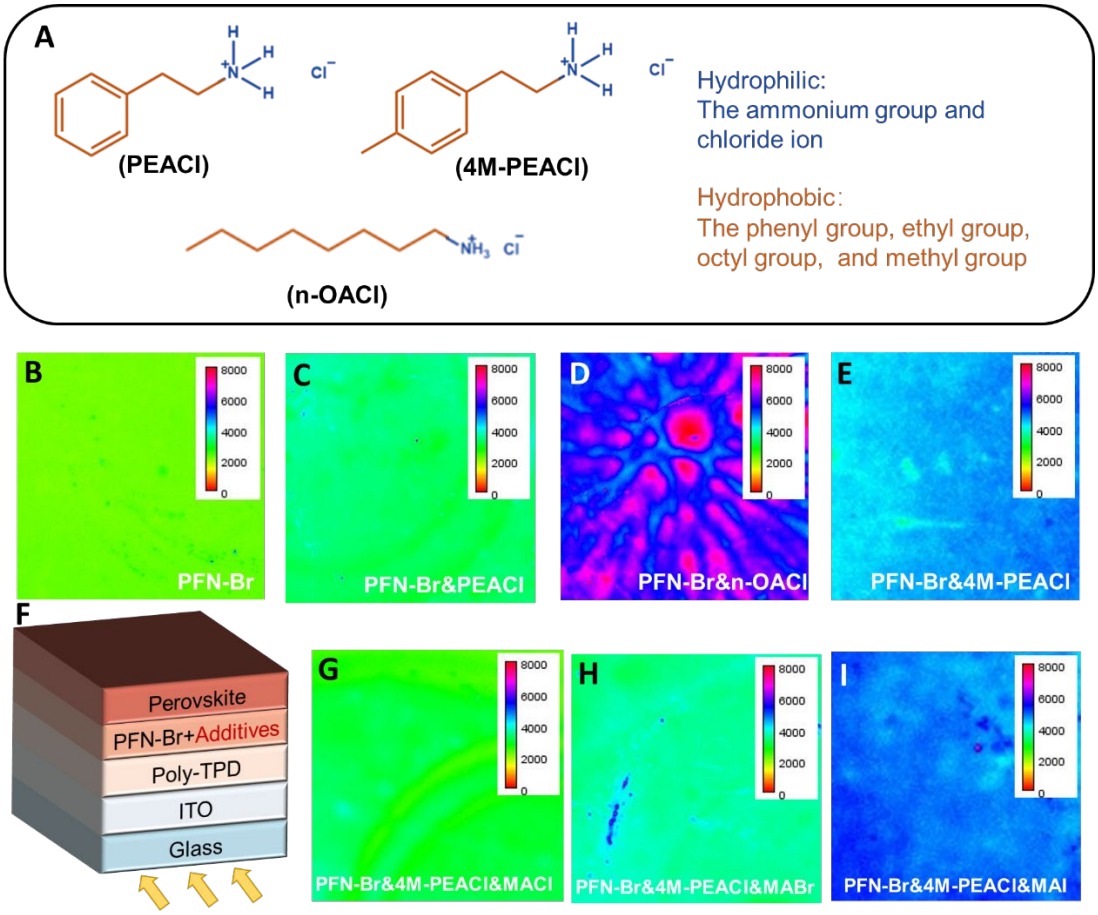

Figure 1 A) Chemical structure of the PEACl, 4M-PEACl, and n-OACl. B-E) Stabilized PL image of perovskite film spin-coated on the different interlayers covering the Poly-TPD/ITO/Glass. F) PL measurement geometry G-I) Stabilized PL image of perovskite film spin-coated on the different interlayers covering the Poly-TPD/ITO/Glass.

To study the influence of ammonium-based salts with different functional groups at the interface between the perovskite and the Poly-TPD, we integrated PEACl, 4M-PEACl, and n-OACl with the PFN-Br. As shown in **Figure 1A**, the chemicals encompass hydrophobic groups that could potentially adhere to the Poly-TPD's surface due to interaction with other hydrophobic groups within the polymer. This may result in an oriented interlayer promoting uniformity with hydrophilic groups oriented upwards. We compared the stabilized photoluminescence (PL) image intensity of perovskite films atop different interlayers (**Figure 1B-E**), including PFN-Br mixed with PEACl, 4M-PEACl, and n-OACl, with the measurement conducted from the glass side (**Figure 1F**). We observed that the ammonium salts combined with the conjugated polymer resulted in enhanced PL intensity, suggesting reduced non-radiative recombination. Interestingly, when MAI was added into 4M-PEACl,

PL intensity further increased, whereas MABr and MACl additives only slightly improved the intensity (**Figure 1G-I**).

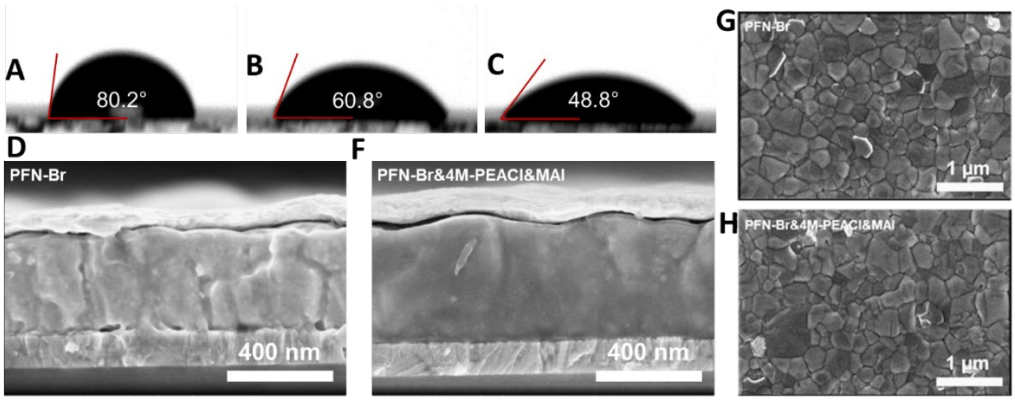

Figure2. Contact angles of water solution droplet on the substrates with (A) No interlayer (B) PFN-Br (C) PFN-Br&4M-PEACl&MAI. D&F) Comparison of the cross-sectional scanning electron microscopy (SEM) images of the perovskite films processed on PFN-Br and PFN-Br&4M-PEACl&MAI films. G&H) Surface morphology SEM images of perovskite films processed on PFN-Br and PFN-Br&4M-PEACl&MAI films.

We measured the water contact angle on different materials on the Poly-TPD surface. As illustrated in **Figure 2A-C**, without surface treatment, Poly-TPD displays poor wettability. The water contact angle decreases when PFN-Br&4M-PEACl&MAI mixture is coated, which improves the wettability. We examined the sample's top surface and cross-section using SEM imaging. As displayed in **Figure 2D&E**, the addition of 4M-PEACl&MAI resulted in a densely packed perovskite film without visible vacancies between the Poly-TPD bottom layer and the perovskite. Furthermore, as demonstrated in **Figure 2G-I**, the additives' presence generally led to an increase in the average grain size of the perovskite.

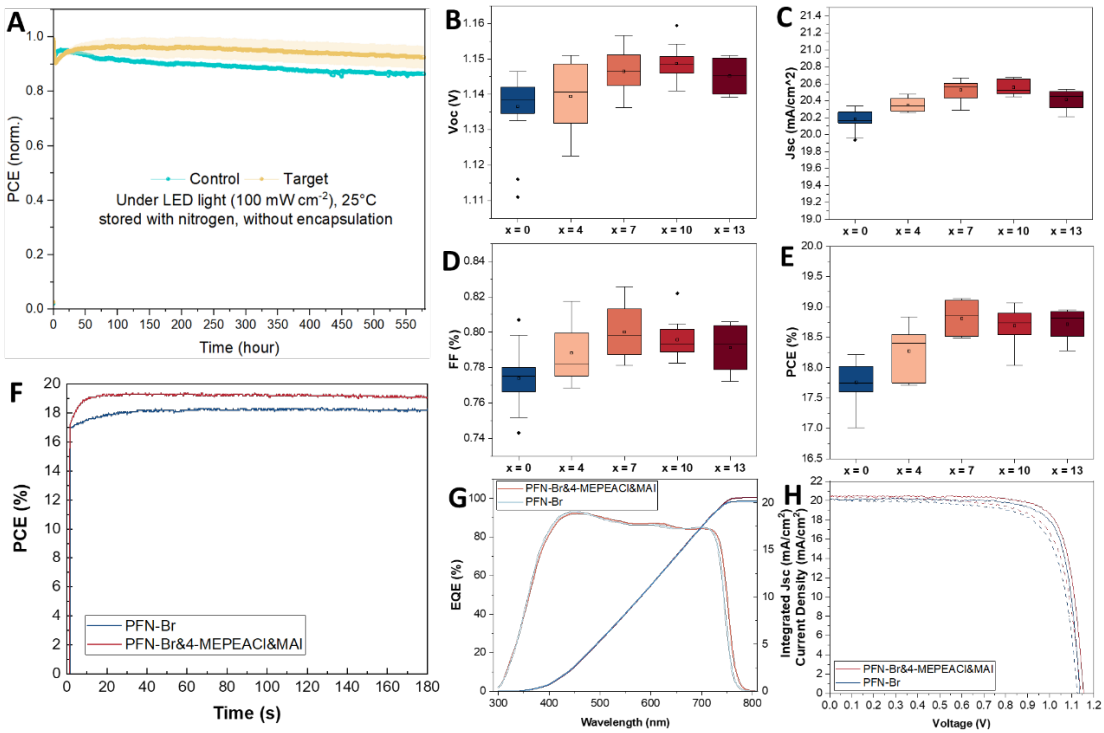

Figure3. A) Light stability test under continuous 1-sun light illumination, the result consisted of 3 samples for each condition B-E) V_{OC}, J_{sc}, *FF* and PCE distribution of PSCs. F) Maximum power point tracking (MPPT) under simulated AM 1.5G illumination G) External quantum efficiency (EQE) spectra of the PFN-Br and PFN-Br&4M-PEACl&MAI based PSCs H) Photovoltaic performance of the PSCs.

We fabricated inverted perovskite solar cell devices based on the PFN-Br&4M-PEACl&MAI mixture with an active area of 0.165 cm². The device configuration is as follows: ITO/Poly-TPD/PFN-Br&4M-PEACl&MAI/$(Cs_{0.22}FA_{0.78})_{0.95}MA_{0.05}Pb(Br_{0.15}I_{0.85})_{0.96}Cl_{0.04}$ (1.68 eV)/C_{60}/BCP/Au. Overall, we observed a general improvement when 4M-PEACl&MAI was added to the system (V_{oc}: 1.16V; *Jsc*: 20.5mA/cm^2; *FF*:80.3%; *PCE*:19.11%) compared to the control device (V_{oc}:1.14V; *Jsc*:20.2mA/cm^2;*FF*:75.2%;*PCE*:17.3%), with an approximate increase in PCE of around 2% absolute value. The improved V_{oc}, J_{sc} and *FF* can be attributed to a more continuous growth of the perovskite on the bottom side with the passivaiton strategy at the bottom.

We conducted the light stability measurement for both the control and target devices with bottom passivation. We observed the improved light stability on the bottom interface modificated deivices remaining 92.5% initial PCE after 550 hours continuous 1-sun illumination. The enhancement in stability can be attributed to the reduction in defects at the interface between the HTL and PVK.

Acknowledgements

This work was supported by the Australian Government through the Australian Renewable Energy Agency (ARENA). Responsibility for the views, information, or advice expressed herein is not accepted by the Australian Government. The authors acknowledge the instruments and expertise of the ACT node of the NCRIS-enabled Australian National Fabrication Facility (ANFF-ACT)

References

1. Lin, Y.-H., et al., *A piperidinium salt stabilizes efficient metal-halide perovskite solar cells.* Science, 2020. **369**(6499): p. 96-102.
2. Zhang, S., et al., *Minimizing buried interfacial defects for efficient inverted perovskite solar cells.* Science, 2023. **380**(6643): p. 404-409.
3. Azmi, R., et al., *Damp heat–stable perovskite solar cells with tailored-dimensionality 2D/3D heterojunctions.* Science, 2022. **376**(6588): p. 73-77.
4. Li, F., et al., *Regulating surface termination for efficient inverted perovskite solar cells with greater than 23% efficiency.* Journal of the American Chemical Society, 2020. **142**(47): p. 20134-20142.
5. Liu, J., et al., *Efficient and stable perovskite-silicon tandem solar cells through contact displacement by MgF x.* Science, 2022. **377**(6603): p. 302-306.
6. Chen, S., et al., *Crystallization in one-step solution deposition of perovskite films: Upward or downward?* Science Advances, 2021. **7**(4): p. eabb2412.
7. Wu, Y., et al., *27.6% Perovskite/c‐Si Tandem Solar Cells Using Industrial Fabricated TOPCon Device.* Advanced Energy Materials, 2022. **12**(27): p. 2200821.
8. Hu, X., et al., *Molecular weight effect of poly-TPD hole-transporting layer on the performance of inverted perovskite solar cells.* Solar Energy, 2021. **218**: p. 368-374.
9. Zhang, F., et al., *Solvent‐Additive Engineering‐Assisted Improvement of Interface Contact for Producing Highly Efficient Inverted Perovskite Solar Cells.* Solar RRL, 2021. **5**(7): p. 2100190.

10. Kim, S., et al., *Interfacial defects change the correlation between photoluminescence, ideality factor, and open‐circuit voltage in perovskite solar cells.* Small, 2021. **17**(33): p. 2101839.
11. Chen, P., et al., *Efficient inverted perovskite solar cells via improved sequential deposition.* Advanced Materials, 2023. **35**(5): p. 2206345.
12. Peng, J., et al., *Interface passivation using ultrathin polymer–fullerene films for high-efficiency perovskite solar cells with negligible hysteresis.* Energy & Environmental Science, 2017. **10**(8): p. 1792-1800.
13. Chen, H., et al., *Quantum-size-tuned heterostructures enable efficient and stable inverted perovskite solar cells.* Nature Photonics, 2022. **16**(5): p. 352-358.